Cement & Concrete Composites 34 (2012) 76–85

Contents lists available at SciVerse ScienceDirect

Cement & Concrete Composites

journal homepage: www.elsevier.com/locate/cemconcomp

Diffusivity and micro-hardness of blended cement materials exposed to external sulfate attack

A. Bonakdar [a], B. Mobasher [a,*], N. Chawla [b]

[a] Civil, Environmental, and Sustainable Engineering, Arizona State University, Tempe, AZ, USA
[b] Materials Science and Engineering, Arizona State University, Tempe, AZ, USA

ARTICLE INFO

Article history:
Received 23 June 2010
Received in revised form 29 August 2011
Accepted 30 August 2011
Available online 8 September 2011

Keywords:
Blended cements
Diffusion
EDS
Micro-hardness
PIXE
Sulfate attack
Reaction

ABSTRACT

Many degradation processes in cement based materials include the diffusion of one or more chemical species into concrete and consequent chemical reactions which alter the chemical and physical nature of the microstructure. External sulfate attack is mostly described by a coupled diffusion–reaction mechanism which leads to the decomposition of hardened cement constituents and cracking of the paste. This paper discusses the significance of diffusion properties and chemical changes in external sulfate attack in blended cement based composites. A method based on Particle Induced X-ray Emission (PIXE) was developed to measure the diffusion properties in a non-destructive test method. Quantitative Energy Dispersive Spectrometry (EDS) and micro-hardness technique were also used to study the chemical and mechanical changes from sulfate attack. Diffusion coefficients and rates of reaction were determined for paste and mortar mixtures, showing higher diffusion rates and lower hardness values in mortar compared to paste for control mixtures. Partial replacement of cement with fly ash improved the transport properties and reduced the level of damage in exposure to sulfate attack.

1. Introduction

1.1. Transport properties in paste and mortar

The durability of cement based materials is directly influenced by the resistance to transport of chemical species throughout the porous multi-component system. External chemical attack involves the transport of aggressive media into concrete via the interaction among various competing mechanisms of ionic diffusion, gas diffusion, liquid sorption, gas permeability, and liquid permeability [1]. The transport properties of concrete have been mostly described by the percolation theory which is based on the idea of connectivity of the pore structure [2].

When concrete is subjected to external sulfate attack, ionic diffusion properties become major indicators of transport characteristics, serviceability, and design life. Sulfate attack proceeds by the diffusion of sulfate ions and inward movement of a reaction front, accompanied by decomposition of major cement paste constituents and formation of expansive products that lead to microcracking of the material [3]. The interfacial transition zone (ITZ) plays an important role in determining the transport properties of the cementitious materials with aggregate inclusions. The characteristic features seen in this zone include higher porosity, larger pores, and higher $Ca(OH)_2$ volume fractions compared to the bulk material [4]. Water permeability of concrete is reported to be as much as 100 times the permeability of its paste component, indicating the dominant role of ITZ [5]. The diffusion coefficients of ITZ have been reported to be 6–12 times more than the bulk cement paste [6,7]. Some ions such as chlorides (Cl^-) and sulfates (SO_4^{-2}) reportedly have similar diffusion rates in normal concrete [8]. The correlation between the transport properties of cement paste and concrete is still controversial and needs more investigation.

1.2. Diffusion equations for cementitious materials

Ionic diffusion is the predominant transport mechanism in most chemical attack cases for cement based materials with Fick's law used as a conventional tool to characterize the process [9,10]. Eq. (1) shows the general 3-D form of Fick's second law for non-steady state (transient) diffusion in Cartesian coordinates, indicating that the rate of change of concentration as a function of time is related to concentration gradient. In the general form of this equation, t is time, (x,y,z) are space coordinates, $C = C(x,y,z,t)$ is the concentration, and $D = D(x,y,z,t,C)$ is the coefficient of diffusion.

$$\frac{\partial C}{\partial t} = \frac{\partial}{\partial x}\left(D\frac{\partial C}{\partial x}\right) + \frac{\partial}{\partial y}\left(D\frac{\partial C}{\partial y}\right) + \frac{\partial}{\partial z}\left(D\frac{\partial C}{\partial z}\right) \quad (1)$$

For most concrete elements with known geometrical shapes and exposure conditions, the simpler 1-D or 2-D problems of diffusion are commonly considered. Since the general mechanism of diffusion of sulfate ions into concrete is similar to the diffusion

* Corresponding author. Tel.: +1 480 965 0141; fax: +1 480 965 0557.
E-mail address: Barzin@asu.edu (B. Mobasher).

0958-9465/$ - see front matter © 2011 Elsevier Ltd. All rights reserved.
doi:10.1016/j.cemconcomp.2011.08.016

Table 1
Values of $R(C)$ for different orders of reaction.

	Zero-order	1st order	2nd order
$R(C)$	k	$k \cdot C$	$k \cdot C^2$ or $k \cdot C_1 \cdot C_2$
Unit of k	Mol S^{-1}	S^{-1}	Mol^{-1} S^{-1}

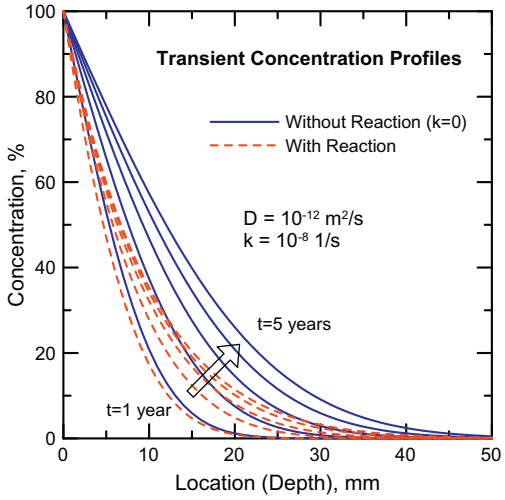

Fig. 1. Concentration profiles for 1-D diffusion with reaction (dashed lines) and without reaction (solid lines). Lines refer to 1–5 years of diffusion.

of chloride ions [8], the formulations for chloride diffusion can be applied to the case of external sulfate attack. However, due to the reaction between penetrating sulfates and existing calcium aluminates (C_3A) in concrete and simultaneous depletion of sulfates, a diffusion–reaction problem should be considered. In this case, the reaction term $R(C)$ is added to the differential equation. Assuming a constant diffusion rate of $D = D_0$, the abovementioned equation will reduce to Eq. (2) for 1-D geometry and Eq. (3) for 2-D geometry with additional reaction terms. The solution to these equations depends on the initial and boundary conditions which are discussed by Crank [10].

$$\frac{\partial C(x,t)}{\partial t} = D_0 \frac{\partial^2 C(x,t)}{\partial x^2} + R(C) \tag{2}$$

$$\frac{\partial C(x,y,t)}{\partial t} = D_0 \left\{ \frac{\partial^2 C(x,y,t)}{\partial x^2} + \frac{\partial^2 C(x,y,t)}{\partial y^2} \right\} + R(C) \tag{3}$$

The reaction can be of different orders, i.e. zero-order, 1st, and 2nd order as described in Table 1. The first two types can be solved using closed-form solutions based on error function or series. The solution to the 2nd order problem needs numerical formulation as expressed by Tixier and Mobasher [11]. A useful case of 1st order reaction for a semi-infinite medium such as a slab or a wall exposed to chemical ingress from one side is discussed here. Given the initial condition of $C(x,0) = C_i$ and boundary condition of $C(0,t) = C_0$, the error function solution is expressed in Eq. (4) for a simplified case of $C_i = 0$. In this equation, D is the apparent coefficient of diffusion and k is the chemical reaction coefficient. Typical concentration profiles (assuming $D = 10^{-12}$ m^2/s and $k = 10^{-8}$ s^{-1}) are shown in Fig. 1 with and without consideration of the reaction term.

$$\frac{C}{C_0} = \frac{1}{2}\left\{ \left[\exp\left(-x\sqrt{\frac{k}{D}} \right) \cdot erfc\left(\frac{x}{2\sqrt{D \cdot t}} - \sqrt{k \cdot t} \right) \right] + \left[\exp\left(x\sqrt{\frac{k}{D}} \right) \cdot erfc\left(\frac{x}{2\sqrt{D \cdot t}} + \sqrt{k \cdot t} \right) \right] \right\} \tag{4}$$

The reported values for coefficients of diffusion for sulfate ions in concrete vary depending on the mixture deigns (aggregate size and volume fraction, pozzolan type, fineness and replacement level, cement fineness, w/cm, additives, etc.) and curing conditions (time, moisture, temperature, etc.). The effective diffusivity can be related to the porosity of cement paste as described by Garboczi and Bentz [12] shown in Eq. (5). In this equation, 'D' is effective ionic diffusivity, 'D_0' is diffusivity of ion in unconfined water, 'φ' is total capillary porosity and $H(x)$ is Heaviside function defined as: $H(x > 0) = 1$ and $H(\leqslant 0) = 0$. Note that D_0 for sulfate ions can be considered in the order of 10^{-9} m^2/s [8]. The reported values for the diffusion coefficients of sulfate ions (D) are in the range of 10^{-14} to 10^{-11} m^2/s for various concrete mixtures [13,14].

$$D = D_0 \cdot \left[H(\varphi - 0.18) 1.8(\varphi - 0.18)^2 + 0.07\varphi^2 + 0.01 \right] \tag{5}$$

The apparent coefficients of diffusion for ions have been traditionally measured by wet chemical methods (e.g. NaCl for chlorides and Na_2SO_4 for sulfates) from a singly exposed side to simulate 1-D diffusion [15]. After sufficient exposure, the sample is drilled and the ground powder is collected at different depths and then subjected to titration. This process is cumbersome and destroys the samples. Non-destructive techniques for elemental analysis may be preferable for studying the transport properties of exposed samples. Determination of the coefficients of diffusion (in 1-D case) is ultimately done by fitting an error function to the concentration profile for the desired elements (Cl^- or SO_4^{2-}) using non-linear regression [15].

Having calculated the coefficient of diffusion and the reaction coefficient for a particular cementitious material, one can use diffusion–reaction based models to predict the level of damage from external sulfate attack. For instance, models proposed by Krajcinovic et al. [16], Tixier and Mobasher [11], and more recently Basista and Weglewski [17] use the diffusion–reaction equations along with the micromechanics of the material to predict the level of expansion and damage. The effect of cracking on the rate of diffusion during the sulfate attack process has been presented in some models such as the works done by Gerard et al. [18] and Gerard and Marchand [19].

Table 2
Test parameters and specifications.

Mix specification	Expansion	PIXE	Micro-hardness	EDS
Specimen size	25 × 25 × 280 mm prisms	50 × 50 mm cylinders	25 × 25 × 10 mm prisms	25 × 25 × 10 mm prisms
Exposure time for testing	Up to 12 months	3 months	3 and 12 months	3 and 12 months
Exposure condition	10% Na_2SO_4 at 25 °C	10% Na_2SO_4 at 75 °C	10% Na_2SO_4 at 25 °C	10% Na_2SO_4 at 25 °C
Mortar				
Control	Yes	Yes	No	No
Blended	Yes	Yes	No	No
Paste				
Control	Yes	Yes	Yes	No
Blended	Yes	Yes	Yes	Yes

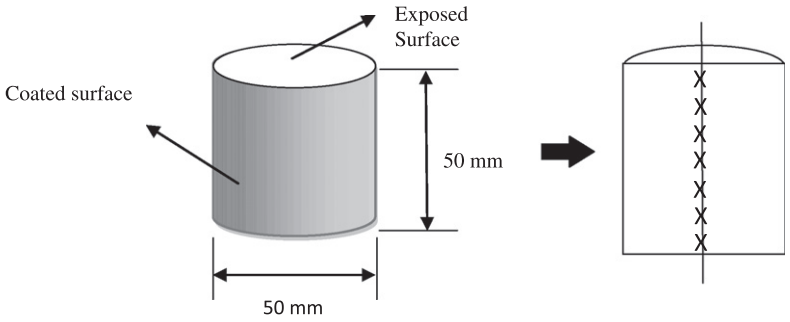

Fig. 2. Schematics of 50 × 50 mm cylinder specimens for 1-D diffusion test. Concentration profiles are obtained for the *X* spots.

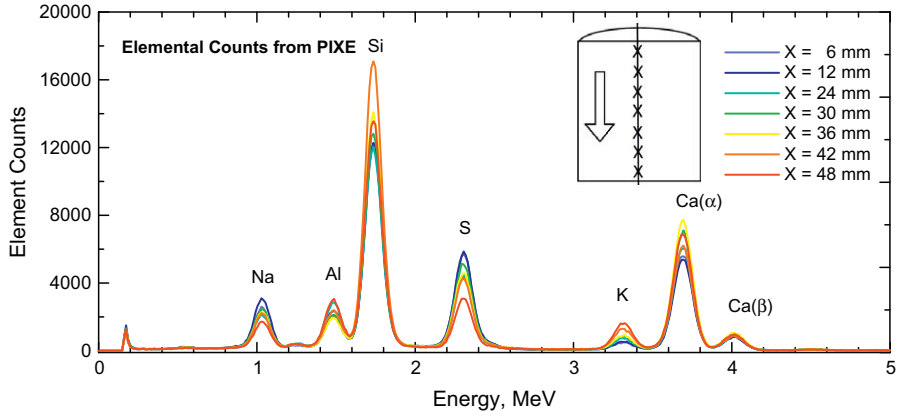

Fig. 3. Typical PIXE result for a specimen exposed to accelerated sulfate attack. Concentration values are obtained for each element for the *X* spots.

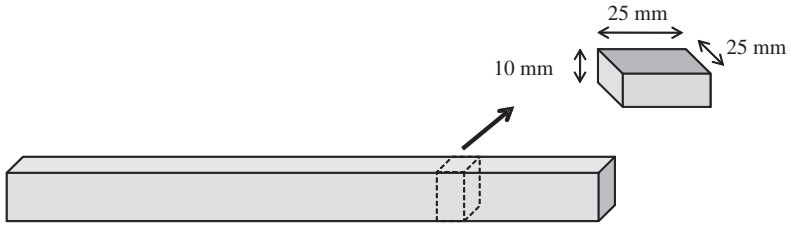

Fig. 4. Schematics of sample preparation for EDS and micro-hardness tests.

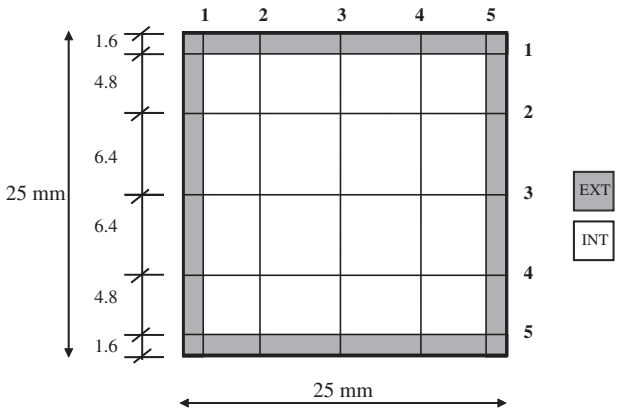

Fig. 5. Grid lines and grid points for EDS and micro-hardness tests. EXT refer to the exterior layer and INT refer to the interior layer for each sample.

1.3. Work objectives

The current work studies the chemical and mechanical changes due to external sulfate attack for some cementitious materials. Paste and mortar mixtures were prepared both for control (Portland cement) and blended cement (class F fly ash). Measurement of the ionic diffusion was performed for major elements and the concentration profiles in 1-D and concentration contours in 2-D were generated. Particle Induced X-ray Emission (PIXE) and Energy Dispersive Spectroscopy (EDS) were used for the measurement of diffusion and chemical changes. One-dimensional diffusion data were compared with the predicted values obtained from diffusion equations. Changes in the macroscopic expansion and micro-hardness were also determined in order to observe the mechanical damage from sulfate attack.

2. Experimental procedure

2.1. Mix designs and test parameters

Four categories of mix designs including paste and mortar with and without fly ash replacement were used for this study. Type I/II Portland cement and low calcium class F fly ash were used with water to cement (W/C) ratio of 0.5 and 28 days of wet-curing prior to testing. Sand to cement (S/C) ratio of 2 was used for mortar mixtures while fly ash to cement (FA/C) ratio of 0.3 was used for blended mixtures. Experiments were conducted to measure the

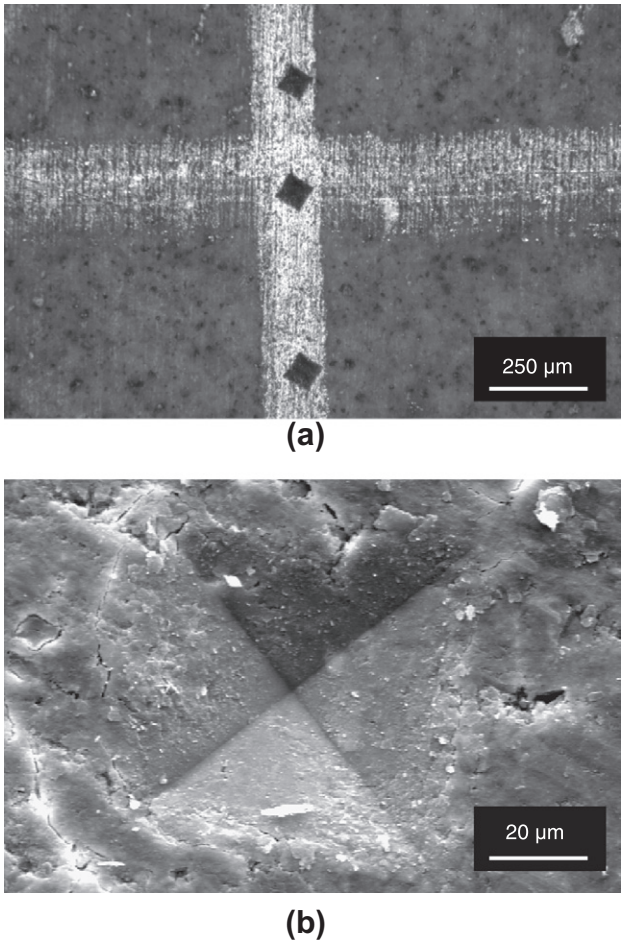

Fig. 6. Indentation images for hardness test using optical microscopy (a) and SEM (b).

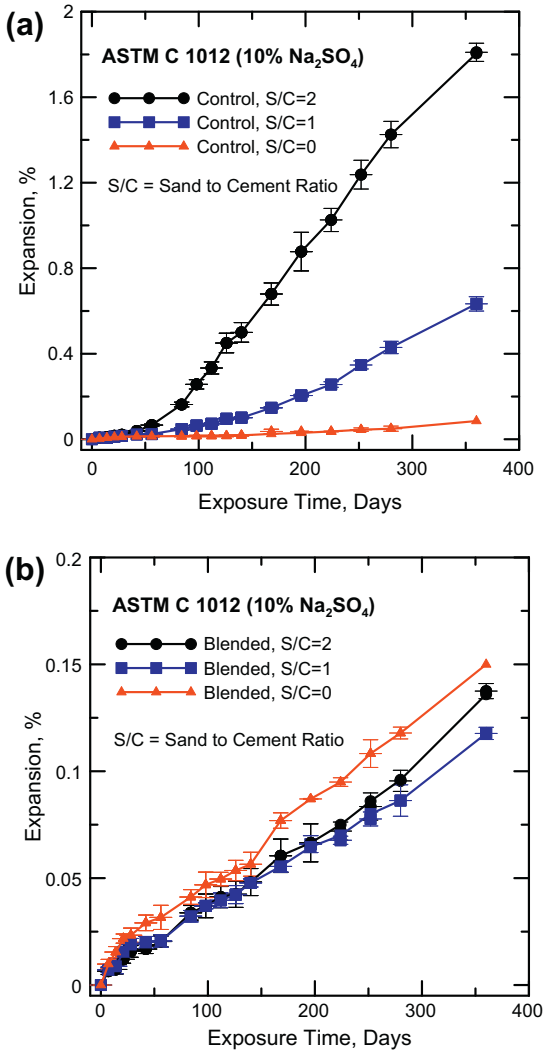

Fig. 7. Linear expansion test results for control mixes (a) and blended mixes (b). Effect of *S/C* ratio is shown for each case.

linear macroscopic expansion, 1-D and 2-D diffusion, and microhardness properties of specimens exposed to sodium sulfate (Na_2SO_4) solution. Different specimen size and exposure conditions were used for different tests as presented in Table 2. It is noted that the current work is a part of a more comprehensive study in a form of dissertation [20] where various types of fly ash (three class F, three class C, and one class N) were used and tested. One particular class F fly ash was selected for this work and the results are presented and compared with the control mixture.

2.2. Linear macroscopic expansion (ASTM C 1012)

Sulfate resistance of cementitious materials has been traditionally tested following ASTM C 1012 [21] in which $25 \times 25 \times 280$ mm prisms are made with cementitious paste or mortar and are exposed to Na_2SO_4 solution at room temperature. Linear length changes (expansions) are measured up to 6–12 months using digital comparators. This test only provides an overall performance of the sulfate resistance and does not determine quantitative measures of transport and mechanical properties. Four replicate specimens were made with paste and mortar mixtures and tested for linear expansion up to 12 months of exposure.

2.3. Particle induced X-ray emission (PIXE)

Particle Induced X-ray Emission (PIXE) is a quantitative and non-destructive technique that relies on the spectrometry of characteristic X-rays emitted when high-energy beams of proton ions (H^+) with 0.3–10 MeV energy ionize atoms of a specimen [22]. PIXE is capable of determining the chemical composition of a bulk sample (with the size order of centimeters) with lateral resolution of 5–2 mm and depth of resolution of 2–30 μm which enables measuring the concentration of a wide range of elements (Na to U) with a resolution down to 1 part per million (ppm) [23]. PIXE has been mostly used for chemical analysis of ancient artifacts and rocks in archeological and geological studies due to its non-destructive nature [24–26].

A test method similar to ASTM C 1556 [15] was used for sample preparation for PIXE test. Paste and mortar mixtures were cast in 50×50 mm cylinders and after curing, the side and bottom surfaces were coated using epoxy as shown schematically in Fig. 2 to permit only a 1-D diffusion profile from the top surface. The specimens were then placed in 10% Na_2SO_4 solution at 75 °C for an accelerated diffusion process. Cylinders were removed from the solution after 3 months of exposure and were cut in two halves using a saw. To obtain the concentration profiles of elements using PIXE, for each half-cylinder, seven spots were scanned with an aperture size of 2 mm along the longitudinal axis. Fig. 3 shows a typical PIXE test result for a variety of major elements (Na, Al, Si, S, K, Ca) obtained for the *X* spots. The concentration profiles of sodium and other elements can then be plotted vs. the depth of penetration for measuring the diffusion coefficients. For verifying the

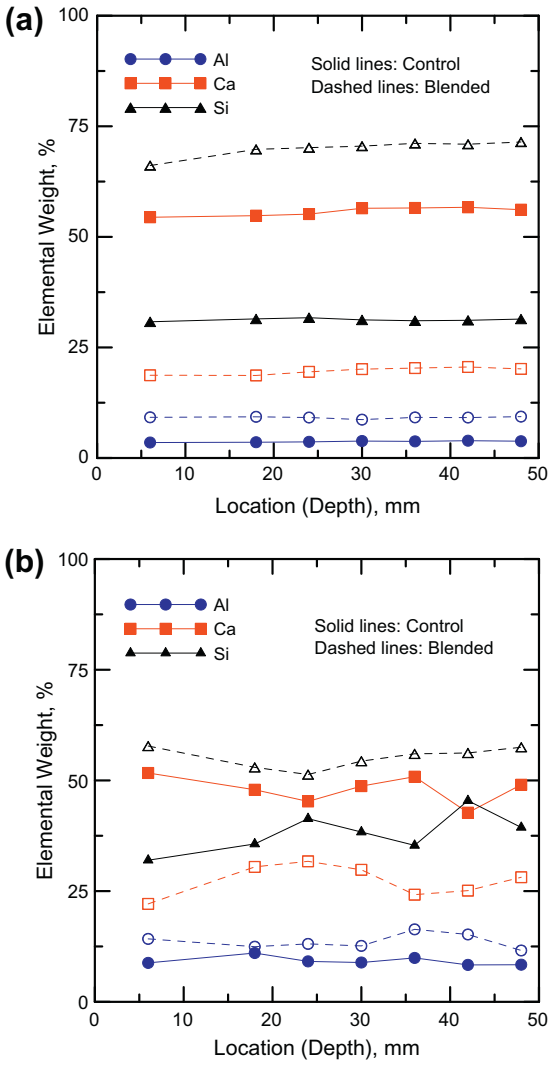

Fig. 8. Concentration profiles of Al, Ca and Si, obtained from PIXE for paste (a) and mortar (b).

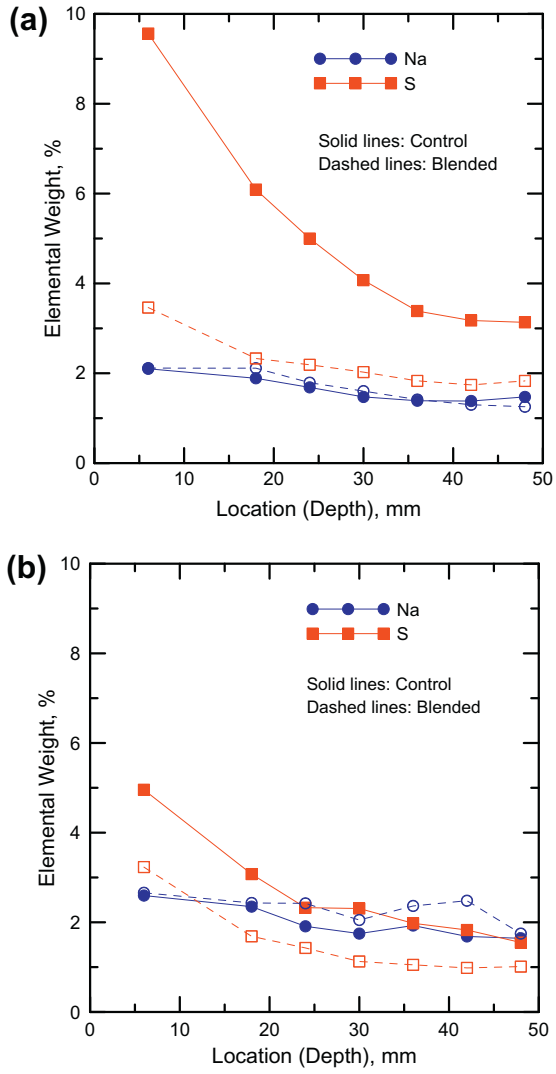

Fig. 9. Concentration profiles of Na and S, obtained from PIXE for paste (a) and mortar (b).

accuracy of PIXE scanning process, specifically in the mortar mixtures where aggregates might affect the results, three palettes were prepared and tested. For this case, samples were drilled at three depths of penetrations (8, 24, and 40 mm); the collected powders were used for making palettes. These palettes with diameter of 10 mm and thickness of 2 mm could be representatives of the overall compositions of the mixture and were made by pressing the ground powder using a hydraulic press.

2.4. Energy dispersive spectroscopy (EDS)

After 12 months of exposure, the 25 × 25 × 280 mm specimens used for the expansion test were also used for chemical analysis using quantitative Energy Dispersive Spectroscopy (EDS). Thin 25 × 25 × 10 mm samples were cut from original specimens exposed to sodium sulfate solution as shown in Fig. 4. These samples were polished using 300 and 600 grit polishing papers and the 25 × 25 mm cross sections were marked using a sharp tipped pencil to generate a grid mesh as schematically shown in Fig. 5. The exterior layer is hereby called EXT and the interior portion is called INT for comparison purposes. A novel SEM-EDS setup was used and the quantitative compositional analyses of exposed samples were obtained using window scanning option with an area of 1 mm^2 for each grid point.

Table 3
Values of D and k calculated from PIXE test.

	Paste ($S/C = 0$)		Mortar ($S/C = 2$)	
	Control	Blended	Control	Blended
D (m^2/s)	5.5×10^{-12}	3.8×10^{-12}	2.4×10^{-11}	1.4×10^{-11}
K (1/s)	3.2×10^{-8}	1.6×10^{-8}	3.2×10^{-8}	1.6×10^{-8}

2.5. Micro-indentation (micro-hardness)

The 25 × 25 × 10 mm thin specimens used for EDS were also used for micro-hardness testing to understand the mechanical changes on the exposed samples. Micro-indentation is a common method of evaluating the quality of materials for engineering purposes, in particular ductile materials (i.e. metals) but also brittle materials such as concrete [27,28]. This technique is based on applying a static load for a known period of time and measuring the response in terms of size of indentation. The Vickers hardness HV (GPa) is calculated per Eq. (6) in which P (Kgf) is the applied force, α is the indenter diagonals angle equal to 136° and D (mm) is the average of diagonals of the indentation [29,30].

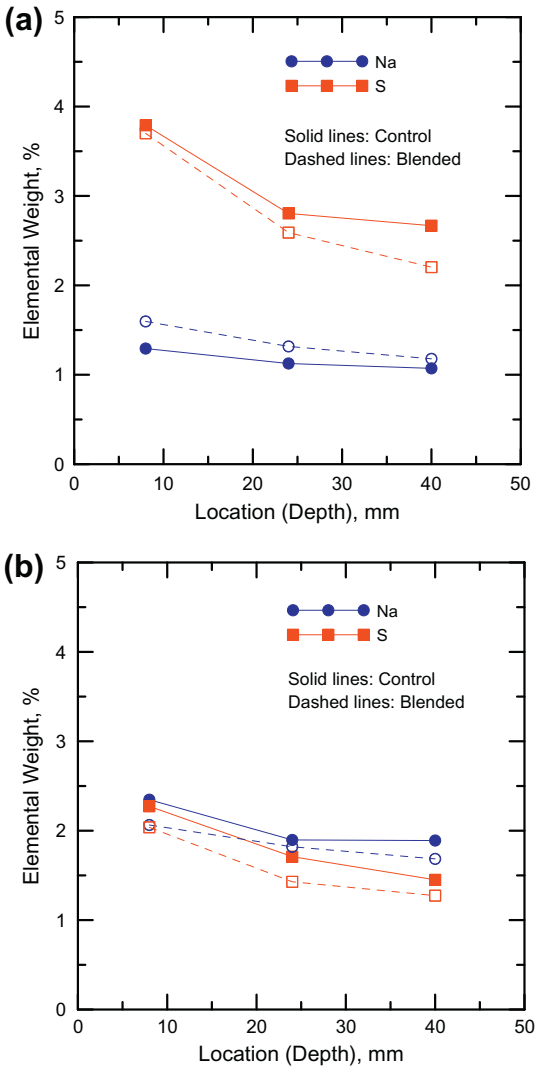

Fig. 10. Concentration profiles of Na and S, using palettes for paste (a) and mortar (b).

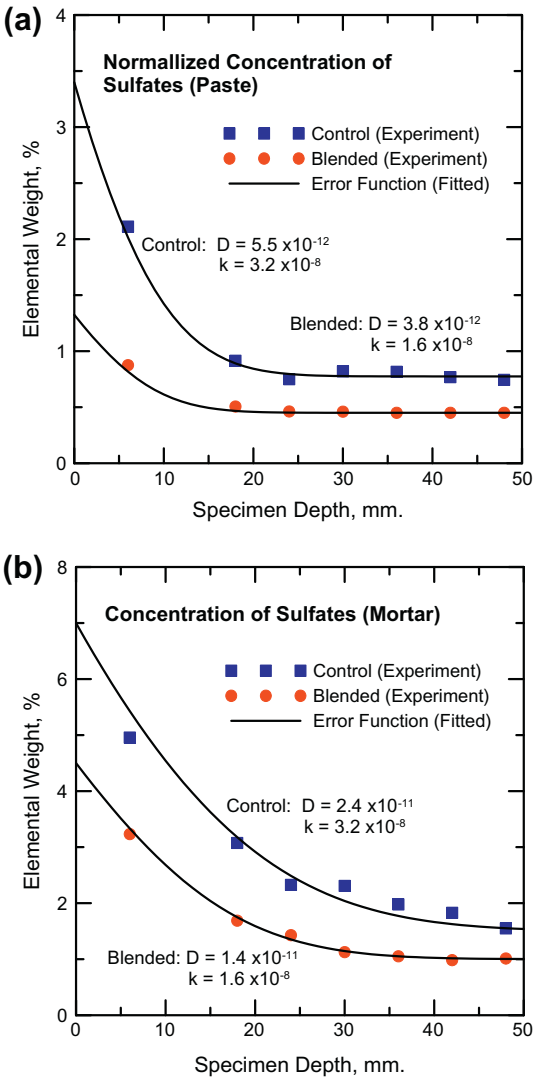

Fig. 11. Concentration profiles and fitted error function with corresponding D and k values for paste (a) and mortar (b).

Table 4
Typical chemical analysis obtained from EDS for blended paste, 12 months exposure.

Point	Location	S	Na	Ca	Si	Al	Mg	O
1-1	EXT	10.7	3.3	18.0	11.6	3.0	0.1	53.3
1-2	EXT	8.9	2.8	18.4	12.5	4.0	0.5	52.8
1-3	EXT	9.9	4.6	17.6	12.2	4.0	0.3	51.4
1-4	EXT	10.6	5.3	17.2	11.4	3.7	0.3	51.6
1-5	EXT	14.4	7.3	14.7	9.1	3.1	0.4	50.9
2-5	EXT	5.4	2.4	20.6	14.2	4.6	0.5	52.3
2-4	INT	2.6	0.9	23.2	16.1	5.2	0.8	51.1
2-3	INT	2.3	0.6	22.8	15.9	5.1	0.5	52.9
2-2	INT	2.5	0.8	22.9	15.8	5.2	0.6	52.1
2-1	EXT	4.7	1.7	21.7	14.4	4.6	0.7	52.2
3-1	EXT	4.7	1.2	22.8	14.7	4.4	0.5	51.8
3-2	INT	2.1	0.8	22.0	15.2	4.8	0.6	54.6
3-3	INT	2.3	0.4	22.7	14.9	4.9	0.5	54.2
3-4	INT	2.2	0.7	22.4	16.1	5.1	0.6	52.9
3-5	EXT	4.1	1.4	21.8	15.0	4.7	0.6	52.4
4-5	EXT	3.7	0.7	22.0	14.9	4.6	0.3	53.7
4-4	INT	2.1	0.7	21.5	15.8	5.1	0.6	54.3
4-3	INT	2.3	0.9	22.9	15.7	5.1	0.8	52.5
4-2	INT	2.2	0.6	21.4	15.2	4.8	0.6	55.1
4-1	EXT	4.2	1.5	20.9	15.0	4.9	0.5	53.0
5-1	EXT	7.6	2.3	19.4	12.8	4.0	0.5	53.4

(*continued on next page*)

Table 4 (*continued*)

Point	Location	S	Na	Ca	Si	Al	Mg	O
5-2	EXT	4.1	3.1	20.8	14.2	4.4	0.4	53.0
5-3	EXT	4.1	3.0	19.2	13.7	4.3	0.5	55.2
5-4	EXT	4.5	3.4	19.9	14.1	4.5	0.4	53.2
5-5	EXT	5.6	3.3	18.8	13.0	4.1	0.5	54.8
Average	EXT	6.7 ± 3.2	3.1 ± 1.7	19.6 ± 2.1	13.3 ± 1.6	4.2 ± 0.5	0.4 ± 0.1	52.8 ± 1.2
	INT	2.3 ± 0.2	0.8 ± 0.1	22.4 ± 0.7	15.7 ± 0.4	5.0 ± 0.2	0.6 ± 0.1	53.2 ± 1.4

$$HV = \frac{2P \cdot Sin(\alpha/2)}{D^2} \times 9.81 \times 10^{-3} \quad (6)$$

In this study, a 0.2 Kgf load was applied on the samples for 15 s, followed by a measurement of indentation size using an optical microscope. For each grid point, three replicate indentations were made as shown in Fig. 6a and the average values were used for calculating the hardness values. Fig. 6b shows an SEM image of the indentation performed on a cement paste sample.

3. Results and discussion

3.1. Macroscopic expansion

The linear expansions for control and blended mixtures are shown in Fig. 7a and b. The overall expansion values obtained for mortars are one order of magnitude larger than those obtained for paste for the control mixtures, implying the role of aggregates in generating higher porosity in ITZ in the absence of fly ash. Where an increase of aggregates fraction increases the expansion

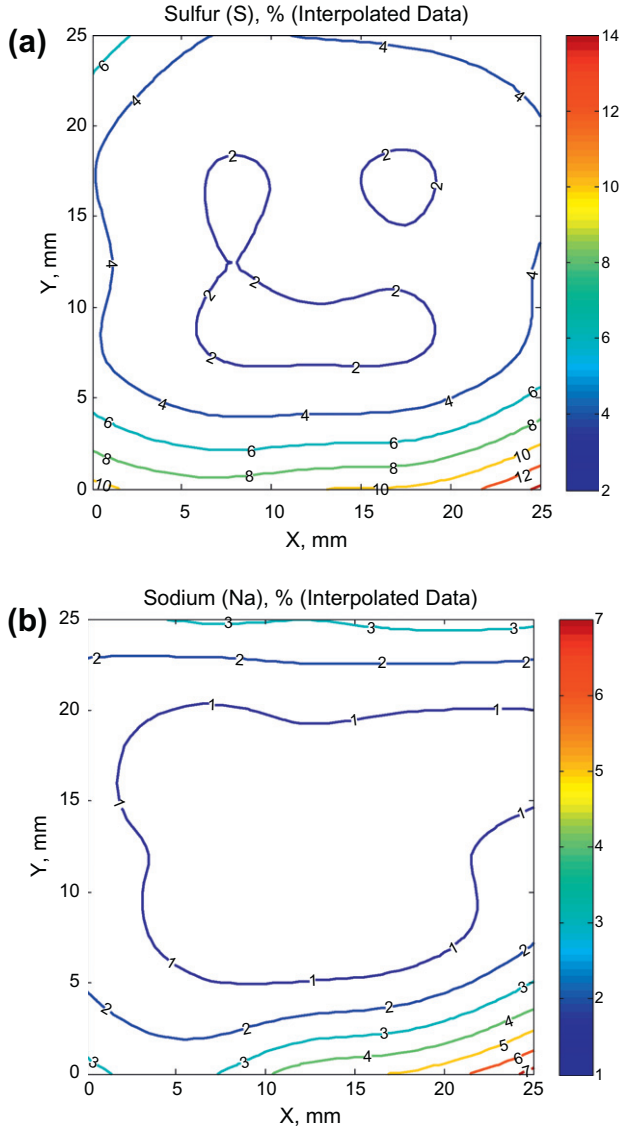

Fig. 12. Contour of chemical compositions obtained from EDS for blended paste mixture for S (a) and Na (b).

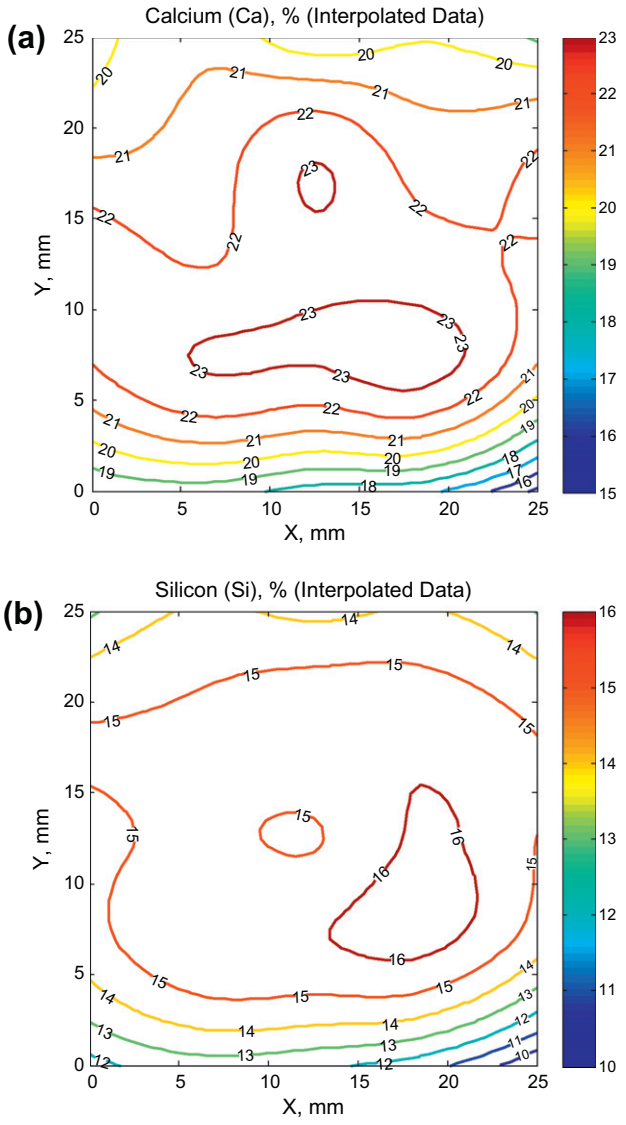

Fig. 13. Contour of chemical compositions obtained from EDS for blended paste mixture for Ca (a) and Si (b).

Fig. 14. Typical one-sided cracking of the 25 × 25 × 280 mm bars, responsible for non-symmetric ionic diffusion.

Table 5
Hardness values (GPa) for control paste, 12 months exposure.

	1	2	3	4	5
1	0.453 ± 0.025	0.526 ± 0.044	0.461 ± 0.077	0.538 ± 0.048	0.458 ± 0.043
2	0.459 ± 0.088	0.460 ± 0.034	0.463 ± 0.044	0.477 ± 0.027	0.469 ± 0.073
3	0.474 ± 0.031	0.505 ± 0.013	0.428 ± 0.047	0.458 ± 0.006	0.438 ± 0.019
4	0.520 ± 0.025	0.409 ± 0.027	0.439 ± 0.036	0.432 ± 0.031	0.472 ± 0.034
5	0.582 ± 0.026	0.534 ± 0.042	0.494 ± 0.019	0.478 ± 0.017	0.535 ± 0.033

for control mixtures, the fly ash blended mixtures seem to be less sensitive to this parameter. This can be explained by the beneficial effect of fly ash in improving the ITZ characteristics. The averaged expansion values vary between 0.1% and 1.8% for control but only 0.1% and 0.15% for blended cement systems.

3.2. Diffusion characteristics

The elemental analyses obtained from PIXE were used and weight percent of the major elements (Ca, Si, Al, Na, and S) were plotted for different depths of penetration. Fig. 8a and b shows the concentration profiles for calcium, aluminum, and silicon for paste and mortar mixtures, after 3 months of exposure. Fly ash blended systems were relatively higher in the levels of Si and Al and lower in Ca contents due to the modification of the overall chemical compositions. The variations of these elements are not significant at various depths of penetration; however paste mixtures show a smoother trend compared to the mortar mixtures. This could be due to relatively short exposure time (3 months) in PIXE test setup. Fig. 9a and b on the other hand present the variations of sodium and sulfur contents in paste and mortar mixtures. The level of Na in control and blended systems are not very different, however the concentrations of S are changing dramatically in the two systems. Fig. 10a and b shows the variations of sodium and sulfur in mortar and paste mixtures obtained from the analysis of powder palettes. The results are in partial agreement with the concentrations obtained from regular (non-destructive) PIXE test setup. It should be noted that this agreement is more reliable for higher depths of penetration (i.e. 40 mm), however for shallower depths (i.e. 10 mm), there is a 4% difference in the concentration values obtained from the two methods.

The concentrations of sulfur were plotted and error function was used for fitting and measuring D and k values. D which is the coefficient of diffusion plays a more significant role in the diffusion reactions compared to k which is the chemical reaction rate. Original experimental data were used for mortar; however, a normalization factor was used for modifying the data for paste mixtures. This is due to the alternation of chemical and porous characteristics in mortar compared to paste from the addition of aggregates. The coefficients of diffusion and rates of reaction are shown in Fig. 11a and b, as well as Table 3 for S/C ratio of 2. The results show that the coefficients of diffusion for mortar mixtures are as much as 3.5–4.5 times higher in mortar compared to paste.

The major elements obtained from EDS (S, Na, Ca and Si) were plotted using interpolated contours on the cross section of the specimens. Table 4 shows the typical results obtained from quantitative EDS for paste blended mixture after 12 months of exposure. The average value of sulfur (S) is 6.7% in the exterior layer but only 2.2% in the interior of the sample. These values are 19.6% and 22.3% for calcium (Ca), implying that this element has leached out of the specimen into the solution. The results are presented graphically for major elements. Fig. 12a and b shows the contour plots for sulfur and sodium, demonstrating the diffusion of these elements while Fig. 13a and b shows the leaching of calcium and silicon outside of the samples. The non-symmetrical distribution of these elements can be attributed to the cracking of the sample on the bottom surface and higher diffusion of

Table 6
Summary of hardness test for all mixtures.

Mixture	Location	Paste		Mortar
		3 Months	12 Months	12 Months
Control	EXT	0.348 ± 0.026	0.493 ± 0.041	0.491 ± 0.110
	INT	0.339 ± 0.023	0.452 ± 0.029	0.557 ± 0.109
	ΔH (%)	+2.6%	+9.1%	−11.8%
Blended	EXT	0.311 ± 0.025	0.406 ± 0.061	0.485 ± 0.091
	INT	0.281 ± 0.027	0.314 ± 0.026	0.493 ± 0.093
	ΔH (%)	+10.6%	+29.3%	−1.6%

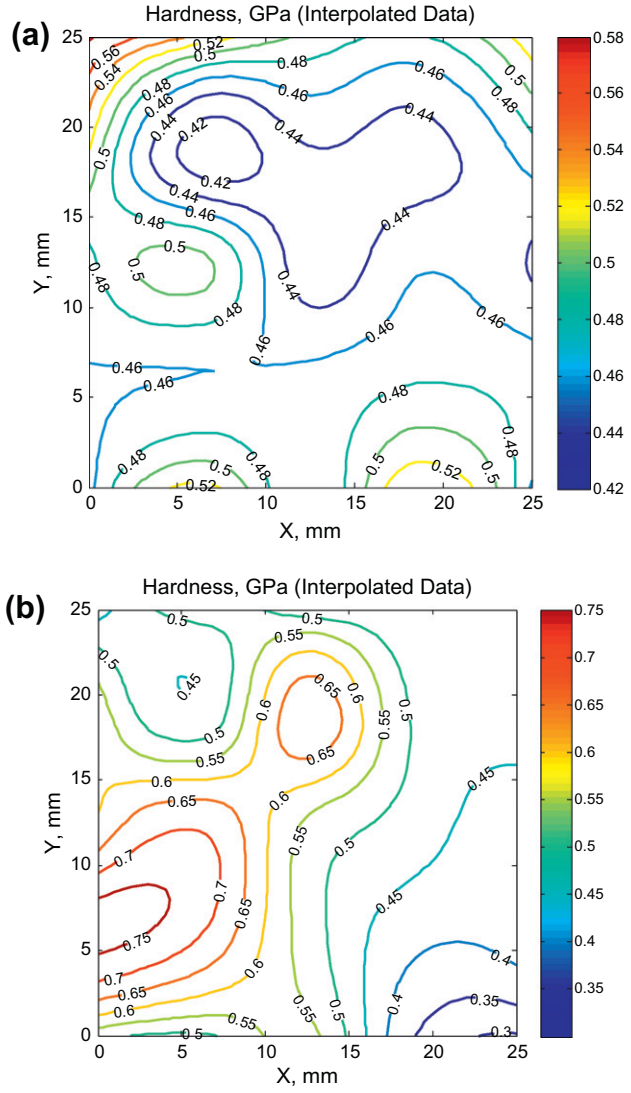

Fig. 15. Hardness contour plots for control paste (a) and control mortar (b) after 12 months.

S and Na, as well as higher leaching of Ca and Si through this surface. The non-symmetry which is explained by one-sided cracks can be observed in most of the exposed specimens and shown typically in Fig. 14.

3.3. Micro-hardness characteristics

The values for micro-hardness were calculated and for one typical case (control paste after 12 months of exposure), presented in Table 5 with each cell representing the average and standard deviation of three indentations (6 diagonals). The average and standard deviations for the exterior (EXT) layer and the interior (INT) layer are presented in Table 6 for all the mixtures along with the percentage of change in hardness value (ΔH). The values corresponding EXT and INT are the basis for comparison in the following statements. The hardness values for paste mixtures increased (EXT vs. INT) as sulfates diffused into the sample and ettringite crystals were formed before cracking took place. This increase was higher in blended systems (10.6% after 3 months and 29.3% after 12 months) compared to the control (2.6% and 9.1%). On the other hand and for mortar mixtures, the hardness has decreased (EXT vs. INT) after 12 months of diffusion in the cracked samples. This reduction is much higher in the control (11.8%) compared to blended (1.6%) after 12 months of exposure. The hardness values are interpolated and represented as surfaces in Fig. 15a and b. This change of response between paste and mortar mixtures is in agreement with the higher diffusion rates and expansion levels of mortar in comparison with paste mixtures.

The results from expansion tests, diffusion tests and microhardness tests were found to be compatible, all indicating lower diffusion rate and less damage in paste mixtures compared to mortar mixtures for control specimens. This can be explained by the effect of interfacial transition zone (ITZ) which exists in mortar due to the presence of aggregates inclusions. Higher porosity and faster diffusion followed by cracking and stiffness reduction was observed in these mixtures. Partial replacement of Portland cement with class F fly ash improved the ITZ, as well as transport properties and reduced the level of damage from sulfate attack.

4. Conclusion

The physical, chemical and mechanical alternations of cement based materials were studied in exposure to external sulfate attack. Paste and mortar mixtures were made with and without fly ash replacement in various specimen forms. The standard ASTM C 1012 test method was followed for measuring the macroscopic linear expansion of the materials which showed that the level of expansion in control mortar mixtures were one order of magnitude higher than the control paste mixtures, possibly due to the ITZ effect in increasing the porosity of the system. Fly ash blended mixtures with improved microstructure were less sensitive to the aggregate addition.

Particle Induced X-ray Emission (PIXE) setup was used for the measurement of concentration profiles of the major elements in a 1-D diffusion problem. Being a non-destructive and fast method, PIXE was found to be a very useful technique. The values of diffusion coefficients were 3.5–4.5 times more in control mortar mixtures compared to the paste mixtures. The 2-D contours of concentration of the major elements obtained from quantitative EDS showed the diffusion of sodium and sulfur and leaching of calcium and silicon during the 12 months of sulfate attack. The microhardness values of the exposed samples were also determined which showed an increase of hardness (2.6–29.3%) in paste mixtures and a decrease of hardness values (1.6–11.8%) in mortar mixtures in the exterior layers. These studies imply an improvement of the microstructure, i.e. less porous ITZ for fly ash blended mixtures.

Acknowledgments

We gratefully acknowledge the use of facilities within the Center for Solid State Science at Arizona State University. The authors also thank Dr. Jason Williams for assistance with specimen preparation and hardness testing. The financial supports of Salt River Project (SRP) and Salt River Materials Group (SRMG) are also appreciated.

References

[1] Bentz DP, Clifton JR, Ferraris CF, Garboczi EJ. Transport properties and durability of concrete: literature review and research plan. NIST IR 6395, Gaithersburg, Maryland; 1999.
[2] Bentz DP, Garboczi EJ. Percolation of phases in a three-dimensional cement paste microstructural model. Cem Concr Res 1991;21:325–44.
[3] Bonakdar A, Mobasher B. Multi-parameter study of external sulfate attack in blended cement materials. J Construct Build Mater 2010;24:61–70.
[4] Scrivener KL. The microstructure of concrete, in materials science of concrete. In: Skalny J, editor. Am Ceram Soc, Westerville; 1990.
[5] Young JF. A review of the pore structure of cement paste and concrete and its influence on permeability, in permeability of concrete. In: Whiting D, Walitt A, editors. ACI SP-108, American Concrete Institute, Detroit; 1988.

[6] Bourdette B, Ringot E, Ollivier JP. Modeling of the transition zone porosity. Cem Concr Res 1995;25:741–51.
[7] Breton D, Ollivier JO, Ballivy G. Diffusivite de ions chloride dans la zone de transition entre pate de ciement et roche granitique, in interfaces in cementitious composites. In: Maso JC, editor. RILEM Proceedings No. 18, E&FN Spon, Great Britain; 1993.
[8] RILEM Report 12. Performance criteria for concrete durability. In: Kropp J, Hilsdorf HK, editors. E&FN SPON, UK; 1995.
[9] Collepardi M, Marcialis A, Turriziani R. Penetration of chloride ions in cement pastes and in concretes. J Am Ceram Soc 1972;55:534–5.
[10] Crank J. The mathematics of diffusion. Oxford: Clarendon Press; 1975.
[11] Tixier R, Mobasher B. Modeling of damage in cement-based materials subjected to external sulfate attack-Part 1: Formulation. ASCE J Mater Civil Eng 2003;15:305–13.
[12] Garboczi EJ, Bentz DP. Diffusivity–porosity relation for cement paste. In: Proceeding from seminar on sulfate attack mechanisms, Quebec, Canada; 1999. p. 259–64
[13] Samson E, Marchand J, Snyder KA. Calculation of ionic diffusion coefficients on the basis of migration test results. Mater Struct 2003;36:156–65.
[14] Cabrera JG, Plowman C. The mechanism and rate of attack of sodium sulfate solution on cement and cement/PFA pastes. Adv Cem Res 1988;1:171–9.
[15] ASTM C 1556. Standard test method for determining the apparent chloride diffusion coefficient of cementitious mixtures by bulk diffusion. American Society for Testing and Materials; 2004.
[16] Krajcinovic D, Basista M, Malliek K, Sumarac D. Chemo-micromechanics of brittle solids. J Mech Phys Solids 1992;40(5):965–90.
[17] Basista M, Weglewski W. Chemically assisted damage of concrete: a model of expansion under external sulfate attack. Int J Damage Mech 2009;18(1):155–75.
[18] Gerard B, Pijaudier-Cabot G, Laborderie C. Coupled diffusion-damage modeling and the implications on failure due to strain localization. Int J Solids Struct 1998;35(31):4107–20.
[19] Gerard B, Marchand J. Influence of cracking on the diffusion properties of cement-based materials. Part 1: Influence of continuous cracks on the steady-state regime. Cem Concr Res 2000;30:37–43.
[20] Bonakdar A. Multi-scale study of durability in blended cement materials, PhD dissertation, Arizona State University; 2010.
[21] ASTM C 1012. Standard test method for length change of hydraulic-cement mortars exposed to a sulfate solution. American society for testing and materials; 2004.
[22] Plymouth MN. Handbook of analytical methods for materials. Plymouth (MN): Materials Evaluation and Incorporation Inc.; 2001; 13–15.
[23] Hohansson AE, Campbell JL. PIXE a novel technique for elemental analysis. John Wiley & Sons; 1988.
[24] Roumié M, Wicenciak U, Bakraji E, Nsouli B. PIXE characterization of lebanese excavated amphorae from jiyeh archeological site. Nucl Instru Methods Phys Res Section B: Beam Interact Mater Atom 2010;268:87–91.
[25] Grave P, Lisle L, Maccheroni M. Multivariate comparison of ICP-OES and PIXE/PIGE analysis of East Asian storage jars. J Archaeolog Sci 2005;32:885–96.
[26] Sie SH. Progress of quantitative micro-PIXE applications in geology and mineralogy. Nucl Instru Methods Phys Res Section B: Beam Interact Mater Atom 1993;75:403–10.
[27] Igarashi S, Bentur A, Mindess S. Microhardness testing of cementitious materials. Adv Cem Based Mater 1996;4:48–57.
[28] Trtik P, Bartos PJM. Micromechanical properties of cementitious composites. Mater Struct 1999;32:388–93.
[29] Meyers MA, Chawla KK. Mechanical behavior of materials. New Jersey: Prentice-Hall Inc.; 1999.
[30] ASTM E 384. Standard test method for microindentation hardness of materials. American society for testing and materials; 2009.